Article

Effects of Nanofillers and Synergistic Action of Carbon Black/Nanoclay Hybrid Fillers in Chlorobutyl Rubber

Tomy Muringayil Joseph [1],*, Hanna J. Maria [2], Martin George Thomas [2], Józef T. Haponiuk [1] and Sabu Thomas [3,4,5],*

1   Department of Polymer Technology, Faculty of Chemistry, Gdańsk University of Technology,
     G. Narutowicza 11/12, 80-233 Gdańsk, Poland; jozef.haponiuk@pg.edu.pl
2   School of Chemical Sciences, Mahatma Gandhi University, Kottayam 686560, Kerala, India;
     hannavidhu@gmail.com (H.J.M.)
3   School of Energy Materials, Inter University Centre for Nanoscience and Technology (IIUCNN),
     Mahatma Gandhi University, Kottayam 686560, Kerala, India
4   Department of Chemical Sciences, University of Johannesburg, Doornfontein,
     Johannesburg P.O. Box 17011, South Africa
5   Trivandrum Engineering Science & Technology Research Park, TC-4/2322, GEM Building, Sreekariyam,
     Trivandrum 695016, Kerala, India
*   Correspondence: tomy.muringayil@pg.edu.pl (T.M.J.); sabuthomas@mgu.ac.in (S.T.);
     Tel.: +48-(57)-2834941 (T.M.J.); +91-(94)-47223452 (S.T.)

Abstract: Nanocomposites based on chlorobutyl rubber (CIIR) have been made using a variety of nanofillers such as carbon black (CB), nanoclay (NC), graphene oxide (GO), and carbon black/nanoclay hybrid filler systems. The hybrid combinations of CB/nanoclay are being employed in the research to examine the additive impacts on the final characteristics of nanocomposites. Atomic force microscopy (AFM), together with resistivity values and mechanical property measurements, have been used to characterise the structural composition of CIIR-based nanocomposites. AFM results indicate that the addition of nanoclay into CIIR increased the surface roughness of the material, which made the material more adhesive. The study found a significant decrease in resistivity in CIIR–nanoclay-based composites and hybrid compositions with nanoclay and CB. The higher resistivity in CB composites, compared to CB/nanoclay, suggests that nanoclay enhances the conductive network of carbon black. However, GO-incorporated composites failed to create conductive networks, which this may have been due to the agglomeration. The study also found that the modulus values at 100%, 200%, and 300% elongation are the highest for clay and CB/clay systems. The findings show that nanocomposites, particularly clay and clay/CB hybrid nanocomposites, may produce polymer nanocomposites with high electrical conductivity. Mechanical properties correlated well with the reinforcement provided by nanoclay. Hybrid nanocomposites with clay/CB had increased mechanical properties because of their enhanced compatibility and higher filler–rubber interaction. Nano-dispersed clay helps prevent fracture growth and enhances mechanical properties even more so than CB.

Keywords: chlorobutyl rubber; CIIR; hybrid fillers; carbon black; nanoclay; graphene oxide; synergistic effects

1. Introduction

Long-chain lightweight polymers offer opportunities for various applications by improving impact strength and stiffness [1–5]. Polymer matrix composites, made from rigid fillers, offer soft, flexible polymer matrices with high toughness due to their easy composition and structural components [6,7]. A composite material is classed as a nanocomposite when one or more dimensions of the added fillers are <100 nm [8]. Nanocomposite materials have been used in the automotive industry [9], but high raw material costs and

production cycle times make them unaffordable for mass production in cost-effective components. Low-volume filler additions to polymer nanocomposites [10,11] improve their marginal contribution and performance in cost and weight through instant processing methods [12]. Interdisciplinary fields are embracing nanoscience and nanotechnology as innovative technologies, with a rapid expansion in rubber nanocomposites. Reinforced rubber improves strength and durability through micro- and nanofiller modifications, ensuring specific end-product properties. Scientists have developed a hybrid nanocomposites technique, combining both organic and inorganic fillers at the nano- or molecular scale in single composites [13,14]. This approach addresses the issue of inorganic materials being highly thermally stable but not very flexible mechanically, while organic materials have weak thermal stability and good mechanical flexibility. The initial research on a polyamide-6 filled with nanoclay by Usuki et al., (1993) and Okada A. (1995) from Toyota R&D is considered the fundamental starting point for understanding this filler behaviour [15,16].

Carbon-based nanofillers like super abrasion furnace (SAF), intermediate super abrasion furnace (ISAF), expanded graphite, Carbon nanotubes (CNTs) and Carbon nanofibers (CNFs) are used to overcome drawbacks in polymer nanocomposite production [17–20]. CNTs are the most cost-effective and economical option, while graphene, the thinnest material in the universe, is a two-dimensional carbon network. In this regard, Hammer's work in 2000 to easily produce GO by oxidizing graphene was groundbreaking [21]. GO has numerous potential applications due to its chemical composition and flake size tunability, including electronics, composites, renewable energy devices, biology, and medicine [22–26]. It is also being considered for electrode materials in batteries, double-layered capacitors, fuel cells, solar cells, and other energy conversion devices [27–30]. CB, another promising reinforcing material, was first used in 1904 as a filler in nanometer and spherical-form composites [31]. It significantly enhances mechanical properties and has since become widely used as a reinforcing material for making rubber composites [32–34]. Dispersed at the nanoscale, CB offers excellent properties for rubbers in industry. Moreover, spherical CB particles may help to reduce the structure inhomogeneity in the nanocomposites. CB and nanoclay interact to enhance tensile modulus and tear strength in nanocomposites [35,36]. This results in reduced air permeability, a reduced water vapour transmission rate, and increased electrical and thermal conductivity in the rubber nanocomposite. However, the high aspect ratio of clay filler causes structure inhomogeneity in rubber/clay composites. The modulus, hardness, and gas barrier properties of the nanocomposite are not significantly affected by inhomogeneity, but they are not ideal for tensile strength and fatigue resistance, due to the high-stress concentration at filler particles and in the unreinforced rubber matrix. It is therefore worthwhile to add CB, a crucial reinforcement filler in the rubber industry, into rubber/clay nanocompounds to improve material properties [37,38].

Polyisobutylene, also known as "butyl rubber", is a type of vinyl elastomer produced through cationic vinyl polymerization of isobutylene with 1–2% isoprene [39]. Butyl rubber is a biocompatible elastomer with excellent damping and ageing properties which is resistant to ketones, phosphate ester, hydraulic fluids, acids, and bases, but not to mineral- or petroleum-based fluids, hydrocarbons, or flame [40]. Butyl rubber offers good insulating properties, making it suitable for use at temperatures ranging from −50 to 250 °F, providing superior resistance against various environmental factors [41]. Because of its low gas permeability, excellent impermeability/air retention, and good flex properties, butyl rubber is reported in various applications [42–44].

Natural rubber (NR) is in widespread use among natural materials, and it is unique for its elasticity among the other materials in general use, making it essential for tyre applications. Even though no synthetic rubber matches the performance of NR, having high elastic properties and tensile strength, it is poor in abrasion resistance, oil and flame resistance, and has poor ageing properties. This is due to the highly unsaturated molecular chain and its non-polar nature. To overcome this problem, we prefer CIIR for this study. In the 1960s, chlorinated and brominated versions (abbreviated as CIIR and BIIR, respectively) were developed, resulting in faster curing times [45–47]. CIIR and BIIR have better gas and

steam impermeability, resistance, and chemical inertia than butyl rubber, which is affected by halogen. CIIR has a chlorine concentration of 1.1% to 1.3% and an unsaturation degree of 1.8 mol [48,49]. CIIR is ideal for pressure marking and rubber combinations because of its high performance in several key areas: low permeability, vibration damping, ageing resistance, and a low glass transition temperature [46,50], and its excellent processing qualities can withstand high temperatures. Despite their limited use in research, CIIR polymers have been reported to exhibit synergistic effects [51,52].

Famous for its airtightness, ozone resistance, and chemical stability, CIIR is also noted for its powerful energy dissipation and combination capabilities. The glass-transition temperature(Tg) of CIIR is reflected in the low shoulder peak of this rubber, while the transition above Tg is the so-called "liquid–liquid transition" (Tll), which can be understood as a delay in the CIIR macromolecular relaxation behaviours necessary for disentanglement or other delayed movements by promissory structures [53]. However, as the largest tan δ peak of CIIR emerges in very low temperatures, its usage as a damping material at room temperature is limited, and it must be blended with other polymers for effective damping. Currently, few studies have reported the filler effect of CIIR, often participating in combined CIIR/NR research [11,54,55]. Breakthrough times were calculated after studying the mechanical, transport, and gas barrier characteristics of CIIR rubber by several researchers, demonstrating its potential use as a barrier material [56,57]. The dynamical behaviour of CIIR was investigated by Fengshun and colleagues [58]. According to the study, the attenuated total reflection and relaxations in the CIIR-rich matrix and AO-80 domains are responsible for the observed relaxations in CIIR/AO-80 blends.

CIIR nanocomposites using CB have been applicable in tyre technology [59], and clays act as gas barrier agents [60,61] in polymer nanocomposites. CIIR-GO, CIIR–clay, and CIIR-CB nanocomposites have potential applications for the manufacturing of inner tubes, inner linings, and tennis balls [54]. The current study presents a new approach to preparing flexible and high-strength elastomeric materials for conductive applications. The focus is on improving interfacial adhesion between components for effective load sharing and mechanical stability. Dispersion behaviour varies due to filler interfaces and geometry. Mechanical analysis was conducted using CIIR for nanocomposites. The study investigates reinforcement and hybrid effects on rubber nanocomposites using CB, clay, GO, and a clay–CB hybrid. It examines the optimal loading for improved properties and maximum synergy. The study also addresses solvent casting techniques for CIIR-based composites, characterizing them using mechanical properties.

2. Materials and Methods

2.1. Materials

The chlorobutyl rubber (CBK 150) with a Mooney viscosity of [ML (1 + 8)@125 °C] of 45, with a chlorine content of 1.2 used in this study, was purchased from Nizhnekamsk, Russia. The organoclay used is I.44P (Nanocor, Houston, Texas, USA; CEC is 70–150 meq/100 g of clay). It is a Montmorillonite modified with an organic modifier octadecyl amine. This was dried for 16 h at 90 °C before use. CB (N-330) was supplied by MRF Tyres. Natural graphite powder was purchased from Sigma Aldrich, Bangalore, Karnataka, India with 99% purity, and the particle size was <20 μm. GO was also used as a nanofiller, and the nanocomposites were prepared using solution casting.

2.2. Graphene Oxide Synthesis

The nanofiller GO was synthesized from natural graphite powder with 99% purity and a particle size of 20 nm, which was purchased from Sigma Aldrich, Bangalore, Karnataka, India. GO was synthesized using a modified Hummers method. The oxygen content of GO produced with this method is typically 30–40% [62].

2.3. Preparation of CIIR Nanocomposite

The study employed the same approach (solution casting) to make each of the five CIIR samples (CIIR pure, CIIR + GO, CIIR + CB, CIIR + clay, and CIIR + CB + clay). A hybrid ultrasonic sonication procedure was used to achieve effective sample dispersion. First, 12 h of constant stirring was carried done to dissolve nanoparticles in toluene. The samples were probe-sonicated in toluene for 5 min at 30% amplitude, for 40 s on and 20 s off. Later, they were bath-sonicated for 12 h before being probe-sonicated again under the aforementioned conditions for improved exfoliation. A magnetic stirrer was used to combine the sample solution with the CIIR in toluene for 24 h. The samples were probe-sonicated for 5 min at 15–20% amplitude, for 40 s on and 20 s off, before and after being subjected to magnetic stirring. Although the sonication process causes high pressure, the off-cycles enabled the temperature to be kept constant to improve the efficiency of sample dispersion. This dispersion method was optimized based on trial and error. Then, the substance was poured into a glass Petri dish and placed in a fume hood at 25 °C for two days. The samples were vacuum-dried at 65 °C for 2 days to remove all traces of solvent. We prepared 1 mm thick nanocomposites using compression moulding.

2.4. Protocol

Different ratios of CIIR nanoparticles were investigated to obtain a sufficient yield for characterization. We dissolved 20 g of CIIR in 300 mL of toluene and kept it for 24 h, before the mixture was mechanically stirred for 3 h. Nanoparticles were diluted to 1% (0.2 g) in toluene (50 mL) and sonicated. The dispersed nanoparticle was added drop by drop to the mechanical stirrer containing CIIR for 4 h, which was then cast in a Petri dish and kept in an oven at 120 °C to evaporate the solvent. Figure 1 shows the schematic depiction of polymer nanocomposites, and the composition used for the study is shown in Table 1.

Table 1. Composition of nanoparticles for CIIR-based composites.

Experiment	Mass of CIIR (Phr)	Mass of Nanoclay (Phr)	Mass of CB (Phr)	Mass of GO (Phr)
CIIR	100	0	0	0
CIIR + CB	100	0	1	0
CIIR + clay	100	1	0	0
CIIR + GO	100	0	0	1
CIIR + clay + CB	100	0.5	0.5	0

2.5. Characterization

Morphological analysis, resistivity, and tensile testing have all been performed to determine the properties of individual nanoparticles. The CIIR nanocomposites were examined using an atomic force microscope using an A-100 SPM (APE Research Nanotechnology, Trieste, Italy) to evaluate the structural changes. The research used platinum-coated cryo-fractured samples prepared by an ion sputter (K575X, Emitech, Fall River, MA, USA). A diamond knife equipped with an ultra-microtome was used to produce ultrathin sections (100 nm thick) of bulk specimens at −10~20 °C. Accurately weighed and sealed samples of 10–15 mg were taken for the study. The AFM images of the cut surface of the samples were taken in tapping mode by the Dimension 3100 Nanoscope, silicon–SPM sensors with a spring constant of ca. 40 N/m and a resonance frequency of 280 kHz were used, with a tip radius of 10 nm, performed by AFM APE research. Resistivity measurement setup (70–530 K) was used to measure the resistance. A universal testing machine (Tinus Olsen-Model H25K-S UTM Benchtop) was used to examine the green strength of CIIR composites. Tensile tests were used to study the mechanical behaviour and were conducted by American Society for Testing and Materials (ASTM) D412-2006. The sample was processed and evaluated by ASTM D6746. The samples were subjected to ASTM D 4180-compliant tensile testing at 23 °C with a cross-head speed of 500 mm/min.
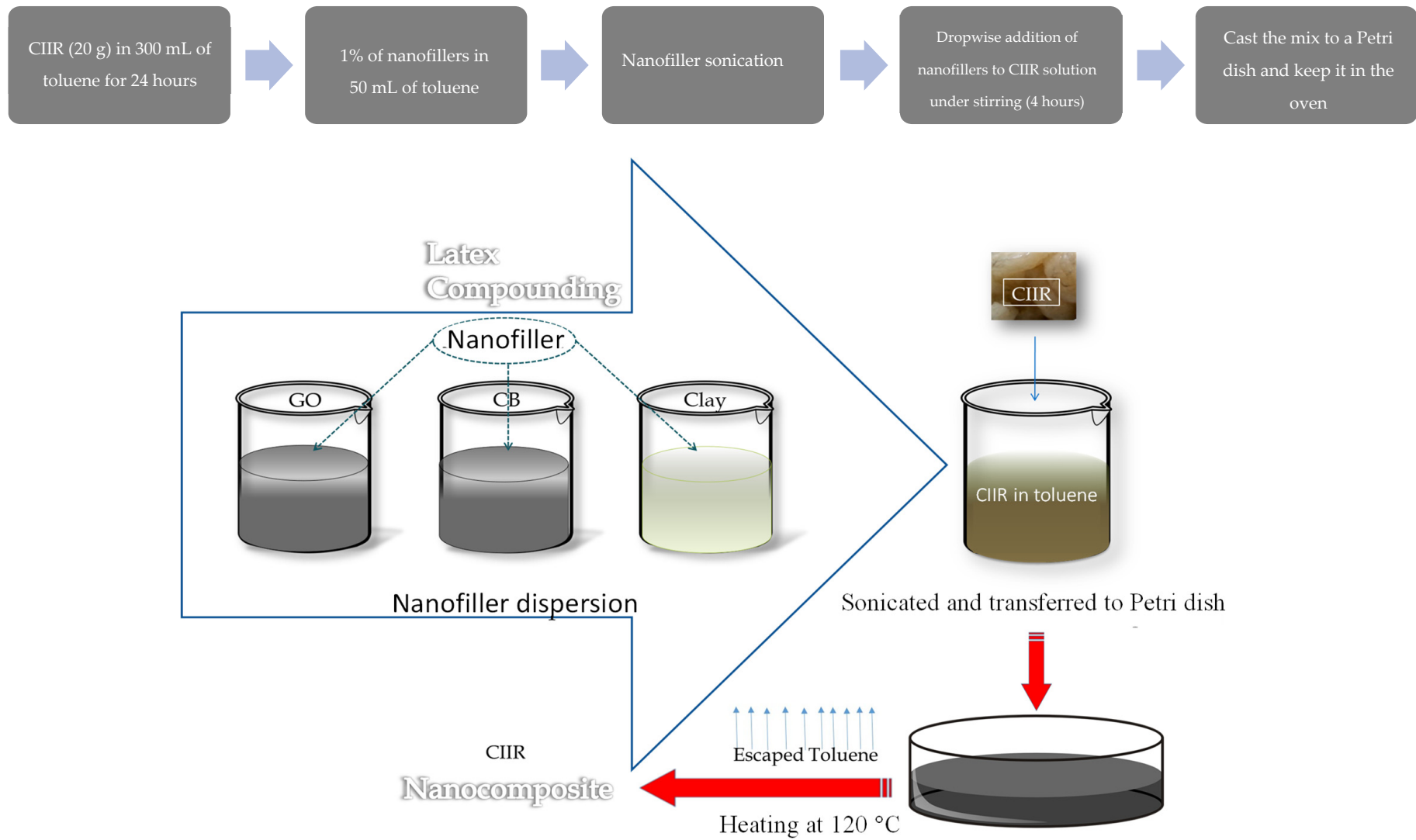
Figure 1. Schematic representation of the preparation of hybrid CIIR nanocomposites.

3. Results and Discussion

3.1. Atomic Force Microscopy

Surface roughness can be measured using Ra and root mean square (RMS), which are two distinct methods. Ra represents the roughness average of microscopic peaks and valleys, while RMS represents the root mean square. Different formulas calculate Ra values based on individual height measurements of surface peaks and valleys, allowing for the comparison of topographic differences between composites by measuring Ra values. We have selected only clay-filled systems and neat CIIR. The AFM images of CIIR and CIIR + clay showed a significant change in morphology with the addition of nanoclay. The addition of nanoclay significantly increased the observed Ra values, approximately four times higher than the neat CIIR. The results indicate that the addition of clay to CIIR increased the surface roughness of the material which made the material more adhesive. Table 2 shows the Ra and RMS values for CIIR + GO and CIIR + clay, and AFM images are shown in Figure 2. We also found that nanoclay was well-dispersed in the CIIR matrix.

Table 2. Ra and RMS for CIIR + clay.

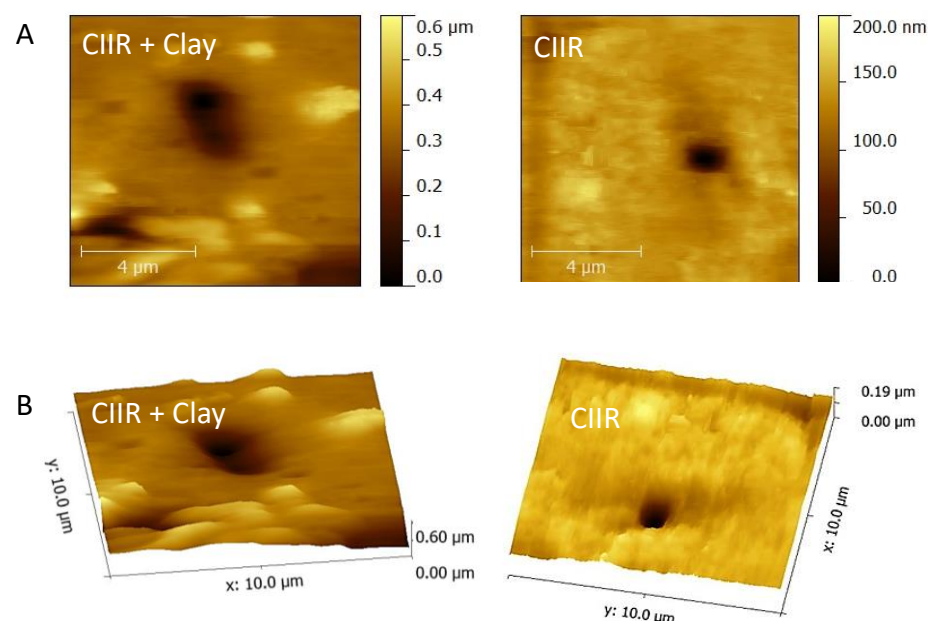|	CIIR	CIIR + Clay
Ra (average surface roughness)	10.88 nm	48.90 nm
RMS (root mean square)	16.88 nm	75.25 nm

Figure 2. AFM images of the CIIR (**A**) and CIIR + clay (**B**).

3.2. Resistivity Measurement

Electrical resistivity is an intrinsic property that quantifies the ability of a given material to oppose the flow of electric current. A substance with a low resistivity enables electric current to flow easily. Resistivity measurements will help develop electrically conductive multifunctional polymer nanocomposites by maintaining the processability and low cost of the starting material. The introduction of electrically conductive fillers into non-conductive polymeric matrixes is one way of improving the conductivity. It has been observed that the addition of carbon-based fillers like graphene, CB, CNT, and carbon fibres to insulating polymers causes a drop in the resistivity of the composite, making it more electrically conductive [63–66].

The effect of nanoclay on the electrical resistivity of various polymer matrices has already been studied [67,68]. From the results, a sharp drop in resistivity is observed

for CIIR–clay-based composites and the hybrid composites with nanoclay and CB. Similar observations were reported by Rashmi et al. in a study based on Montmorillonite nanoclay filler effects on the electrical conductivity of epoxy-based nanocomposites [69]. Experimental results showed that the inclusion of 2 wt% MMT nanofiller increased the Tg, electrical conductivity, thermal stability, modulus, and free volume of the epoxy nanocomposite significantly.

In composites with CB and clay (hybrid systems), the resistivity was higher than in clay-filled systems; however, much lower than CB- and graphene-filled systems. This demonstrates that the addition of nanoclay results in a conductive network due to enhanced CB dispersion. However, for the GO-incorporated composites, the high inherent electrical conductivity and large surface area of GO sheets were not effective in making a conductive network. This could be due to the poor dispersion of GO in the CIIR. Figure 3 displays the resistivity values of CIIR polymer nanocomposites with varying compositions, and Table 3 shows the resistivity values of the composites.
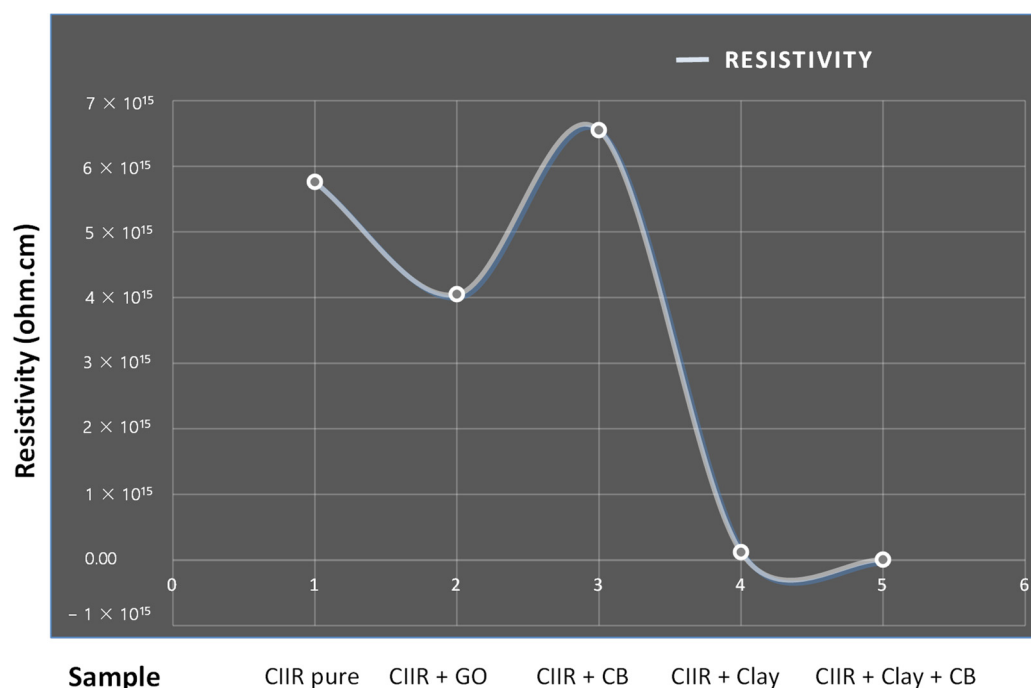

Figure 3. Resistivity values of different compositions of CIIR nanocomposites.

Table 3. Resistivity values of the composites.

Sample	CIIR pure	CIIR + GO	CIIR + CB	CIIR + Clay	CIIR + Clay + CB
Resistivity (Ω-cm)	5.76×10^{15}	4.05×10^{15}	6.55×10^{15}	1.20×10^{14}	3.69×10^{12}

The study reveals that the resistivity decreases in general with the filler loading combinations of CIIR matrixes. The resistivity seems to decrease with an increase in all filler loadings. This decrease in resistivity could be attributed to the hopping phenomenon of conduction theory. The enhanced frequency of the AC electric field increases the flow of the current across the system. In general, the conductivity of filled polymer composites is governed by both the mechanism of conduction theory (the formation of continuous conductive networks) and the hopping mechanism (electric field radiation) of conduction theory [70–72]. Before percolation, the conductivity in the polymer composite is due to the hopping (jumping) of electrons from one conducting site to another, which is facilitated as the distance among the conducting sites is reduced. Thus, with the increase in frequency, the electrons present in the system acquire more energy, which facilitates them hopping

from one conductive site to another, thereby reducing the electrical resistivity. This is due to the formation of continuous conductive filler networks in the polymer matrix. If the continuous conductive network is formed in the polymer matrix, electrons jumping from one conductive site to another is not necessary. Accordingly, the impact of the hopping phenomenon is reduced, which makes it frequency-independent.

The electrical properties of nanocomposites rely on how the filler particles are dispersed through the polymer matrix. At low levels of filler loading, the resistivity of the nanocomposite is slightly lower than that of the base polymer, since the filler particles begin to be in contact with each other, and a continuous path is formed through the volume of the sample for electrons to travel. It was noted by researchers that the material produced directly from GO is not particularly useful as a conductor [73,74]. A partial reduction of GO might be necessary to restore conductivity [75,76]. The report also shows that GO films show poor conductivity at a low humidity, acting as an insulator, but an increase in conductivity at a high humidity, due to enhanced ion conduction [77].

3.3. Mechanical Properties

The stress–strain curve is given in Figure 4. The CB-filled system showed the highest tensile strength (TS) (Figure 4). CB–clay hybrid fillers in CIIR composites have enabled dramatic synergistic reinforcing concerning the modulus (Figure 4 and Table 4), although the TS is lower.
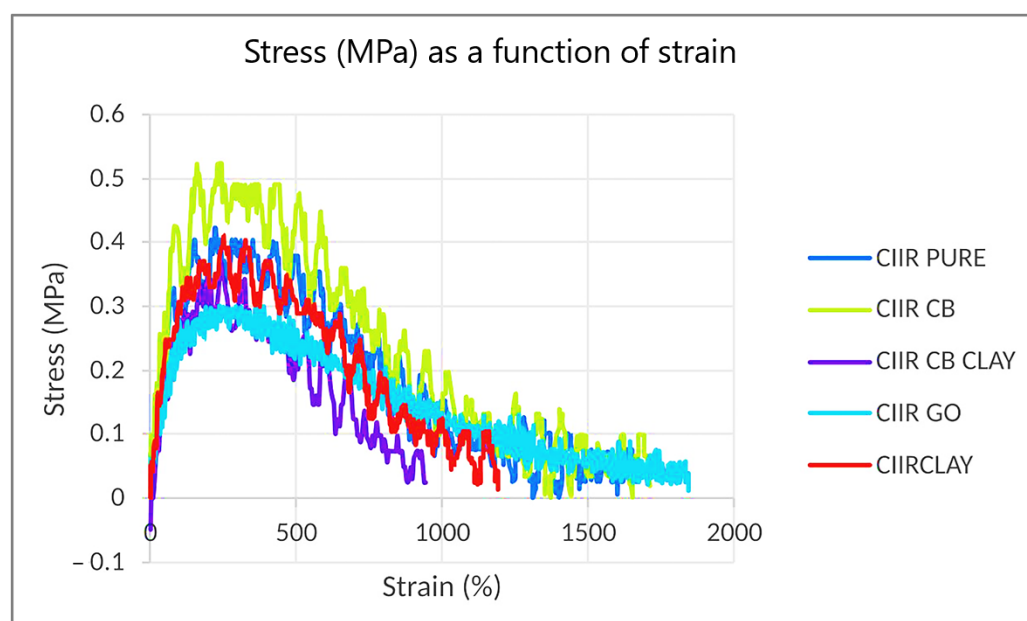

Figure 4. Strain vs. stress for NR composites for different fillers.

Mechanical characteristics were shown to be enhanced in all nanocomposites when compared to pure CIIR. Hybrid composites showed a higher modulus than conventional nanocomposites. This is indicative of the synergistic action of nanoclay and CB. Strong filler–filler and filler–rubber interactions were primarily responsible for the enhanced mechanical characteristics of CIIR/CB composites [63]. The filler dispersion is crucial at high filler loadings. We hypothesize that the highest tensile strength is due to the improved dispersion of CB in CIIR. As can be seen in Figure 5, the carbon black and clay (hybrid system) form a network in the CIIR matrix, nd this leads to the highest modulus values and better conductivity.

We would like to add that all the samples prepared for the study were unvulcanised and, therefore, green strength measurement was critical. To avoid the effect of vulcanization on the reinforcement, we focussed on the unvulcanised green materials. An green strength assessment is crucial for evaluating the mechanical performance of unvulcanised rubber

compounds, especially in CIIR nanocomposites with low concentrations of fillers like CB, GO, and clay. Unvulcanised rubber made using solution casting has a low mechanical strength due to the absence of cross-linking. Dispersed fillers in rubber enhance its mechanical properties due to superior rubber–filler and filler–filler interactions. CB, with its high surface area and network formation capabilities, provides physical reinforcement. GO and clay, with their high aspect ratios and interconnected structures, further strengthen the mechanical strength of the rubber matrix. These fillers contribute to the overall strength of the rubber matrix. Interactions of CB and clay with CIIR are shown schematically in Figure 5.
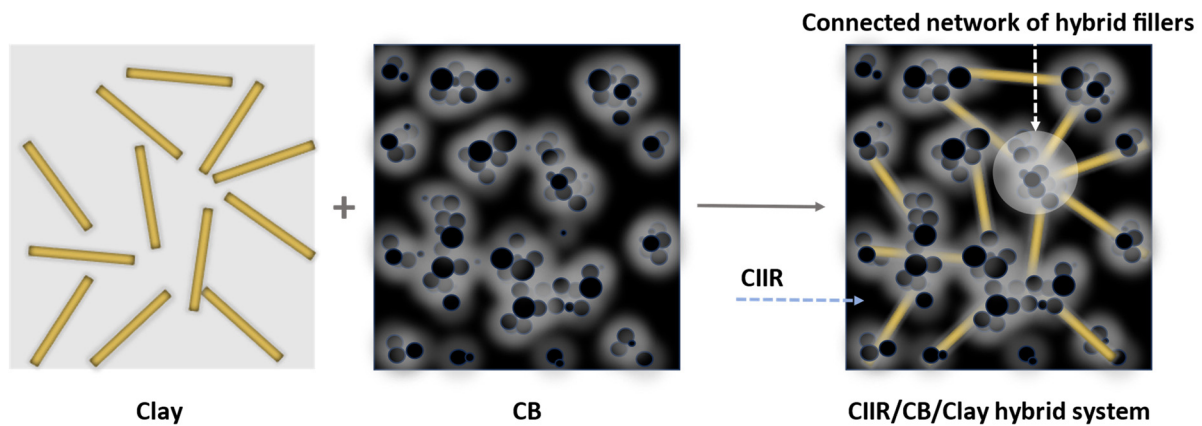

Figure 5. Schematic representation showing the interaction of CB and clay with CIIR.

Table 4. Stress values at 100, 200, and 300 percentage strains of CIIR composites.

(MPa)	CIIR Pure	CIIR/GO	CIIR/CB	CIIR/Clay	CIIR/CB/Clay
Stress at 100% strain	0.27	0.36	0.36	0.44	0.45
Stress at 200% strain	0.35	0.47	0.45	0.53	0.53
Stress at 300% strain	0.36	0.47	0.44	0.53	0.54

4. Conclusions

The study explores the development and characterization of nanocomposites made from CIIR and CIIR/CB/clay hybrid systems. AFM results indicate that the addition of nanoclay to CIIR increased the surface roughness of the material, which made the material more adhesive. The study found a significant decrease in resistivity in CIIR–clay-based composites and in hybrid composites with nanoclay and CB. The higher resistivity in CB composites suggests that nanoclay enhances conductive networks. However, GO-incorporated composites struggled to create conductive networks, and this may have been due to the agglomeration. The study also found that only CB/clay hybrid system showed the highest modulus at 100%, 200%, and 300% elongation, while other nanofillers do not significantly impact these values. Finally, we conclude that hybrid filler systems and advanced characterization methodologies will provide insights into structure-property relationships, facilitating their adoption across various industrial and automotive sectors.

Author Contributions: T.M.J.: conceptualization, methodology, investigation, writing—original draft preparation, and writing—review and editing; H.J.M.: data curation and writing—review and editing; M.G.T.: data curation and writing—review and editing; J.T.H.: supervision and writing—review and editing; S.T.: visualization, writing—review and editing, supervision, and project administration. All authors have read and agreed to the published version of the manuscript.

Data Availability Statement: The original contributions presented in the study are included in the article, further inquiries can be directed to the corresponding authors.

Conflicts of Interest: The authors declare no conflict of interest.

References

1. Ritchie, R.O. The Conflicts between Strength and Toughness. *Nat. Mater.* **2011**, *10*, 817–822. [CrossRef]
2. Suresh, K.I.; Nutenki, R.; Joseph, T.M.; Murali, S. Structural, Molecular and Thermal Properties of Cardanol Based Monomers and Polymers Synthesized via Atom Transfer Radical Polymerization (ATRP). *J. Macromol. Sci. Part A* **2022**, *59*, 403–410. [CrossRef]
3. Joseph, T.M.; Pallikkunnel, M.L.; Mahapatra, D.K.; Kallingal, A.; Thomas, S.; Haponiuk, J.T. Polyurethane−Epoxy Composites: Recent Developments and Future Perspectives. In *Polyurethane Chemistry: Renewable Polyols and Isocyanates*; ACS Symposium Series; American Chemical Society: Washington, DC, USA, 2021; Volume 1380, pp. 257–280, ISBN 978-0-8412-9840-8.
4. Muringayil Joseph, T.; Murali Nair, S.; Kattimuttathu Ittara, S.; Haponiuk, J.T.; Thomas, S. Copolymerization of Styrene and Pentadecylphenylmethacrylate (PDPMA): Synthesis, Characterization, Thermomechanical and Adhesion Properties. *Polymers* **2020**, *12*, 97. [CrossRef]
5. Joseph, T.M.; Kallingal, A.; Suresh, A.M.; Mahapatra, D.K.; Hasanin, M.S.; Haponiuk, J.; Thomas, S. 3D Printing of Polylactic Acid: Recent Advances and Opportunities. *Int. J. Adv. Manuf. Technol.* **2023**, *125*, 1015–1035. [CrossRef] [PubMed]
6. Barreira-Pinto, R.; Carneiro, R.; Miranda, M.; Guedes, R.M. Polymer-Matrix Composites: Characterising the Impact of Environmental Factors on Their Lifetime. *Materials* **2023**, *16*, 3913. [CrossRef] [PubMed]
7. Fan, Q.; Duan, H.; Xing, X. A Review of Composite Materials for Enhancing Support, Flexibility and Strength in Exercise. *Alex. Eng. J.* **2024**, *94*, 90–103. [CrossRef]
8. Reduwan Billah, S.M. Composites and Nanocomposites. In *Functional Polymers*; Jafar Mazumder, M.A., Sheardown, H., Al-Ahmed, A., Eds.; Springer International Publishing: Cham, Switzerland, 2019; pp. 1–67, ISBN 978-3-319-92067-2.
9. Chowdhury, M.I.S.; Autul, Y.S.; Rahman, S.; Hoque, M.E. 11—Polymer Nanocomposites for Automotive Applications. In *Advanced Polymer Nanocomposites*; Hoque, M.E., Ramar, K., Sharif, A., Eds.; Woodhead Publishing in Materials; Woodhead Publishing: Sawston, UK, 2022; pp. 267–317, ISBN 978-0-12-824492-0.
10. Jose Varghese, R.; Vidya, L.; Joseph, T.M.; Gudimalla, A.; Harini Bhuvaneswari, G.; Thomas, S. Potential Applications of XLPE Nanocomposites in the Field of Cable Insulation. In *Crosslinkable Polyethylene Based Blends and Nanocomposites*; Thomas, J., Thomas, S., Ahmad, Z., Eds.; Materials Horizons: From Nature to Nanomaterials; Springer: Singapore, 2021; pp. 197–213, ISBN 9789811604850.
11. Muringayil Joseph, T.; Mariya, H.J.; Haponiuk, J.T.; Thomas, S.; Esmaeili, A.; Sajadi, S.M. Electromagnetic Interference Shielding Effectiveness of Natural and Chlorobutyl Rubber Blend Nanocomposite. *J. Compos. Sci.* **2022**, *6*, 240. [CrossRef]
12. Yuvaraj, G.; Ramesh, M.; Rajeshkumar, L. Carbon and Cellulose-Based Nanoparticle-Reinforced Polymer Nanocomposites: A Critical Review. *Nanomaterials* **2023**, *13*, 1803. [CrossRef]
13. Raman, N.; Sudharsan, S.; Pothiraj, K. Synthesis and Structural Reactivity of Inorganic–Organic Hybrid Nanocomposites—A Review. *J. Saudi Chem. Soc.* **2012**, *16*, 339–352. [CrossRef]
14. Jaafar, M. Development of Hybrid Fillers/Polymer Nanocomposites for Electronic Applications. In *Hybrid Nanomaterials*; John Wiley & Sons, Ltd.: Hoboken, NJ, USA, 2017; pp. 349–369, ISBN 978-1-119-16038-0.
15. Okada, A.; Usuki, A. The Chemistry of Polymer-Clay Hybrids. *Mater. Sci. Eng. C* **1995**, *3*, 109–115. [CrossRef]
16. Usuki, A.; Kojima, Y.; Kawasumi, M.; Okada, A.; Fukushima, Y.; Kurauchi, T.; Kamigaito, O. Synthesis of Nylon 6-Clay Hybrid. *J. Mater. Res.* **1993**, *8*, 1179–1184. [CrossRef]
17. Ke, K.; Yue, L.; Shao, H.; Yang, M.-B.; Yang, W.; Manas-Zloczower, I. Boosting Electrical and Piezoresistive Properties of Polymer Nanocomposites via Hybrid Carbon Fillers: A Review. *Carbon* **2021**, *173*, 1020–1040. [CrossRef]
18. Dassan, E.G.B.; Rahman, A.A.A.; Abidin, M.S.Z.; Akil, H.M. Carbon Nanotube–Reinforced Polymer Composite for Electromagnetic Interference Application: A Review. *Nanotechnol. Rev.* **2020**, *9*, 768–788. [CrossRef]
19. Syduzzaman, M.; Chowdhury, K.P.; Fahmi, F.F.; Rumi, S.S.; Hassan, A. Effects of Carbon-Based Nanofillers on Mechanical, Electrical, and Thermal Properties of Bast Fiber Reinforced Polymer Composites. *J. Thermoplast. Compos. Mater.* **2023**, 08927057231216740. [CrossRef]
20. Zhou, X.; Wang, Y.; Gong, C.; Liu, B.; Wei, G. Production, Structural Design, Functional Control, and Broad Applications of Carbon Nanofiber-Based Nanomaterials: A Comprehensive Review. *Chem. Eng. J.* **2020**, *402*, 126189. [CrossRef]
21. Zaaba, N.I.; Foo, K.L.; Hashim, U.; Tan, S.J.; Liu, W.-W.; Voon, C.H. Synthesis of Graphene Oxide Using Modified Hummers Method: Solvent Influence. *Procedia Eng.* **2017**, *184*, 469–477. [CrossRef]
22. Singh, D.P.; Herrera, C.E.; Singh, B.; Singh, S.; Singh, R.K.; Kumar, R. Graphene Oxide: An Efficient Material and Recent Approach for Biotechnological and Biomedical Applications. *Mater. Sci. Eng. C* **2018**, *86*, 173–197. [CrossRef] [PubMed]
23. Priyadarsini, S.; Mohanty, S.; Mukherjee, S.; Basu, S.; Mishra, M. Graphene and Graphene Oxide as Nanomaterials for Medicine and Biology Application. *J. Nanostructure Chem.* **2018**, *8*, 123–137. [CrossRef]
24. Devi, N.; Kumar, R.; Singh, S.; Singh, R.K. Recent Development of Graphene-Based Composite for Multifunctional Applications: Energy, Environmental and Biomedical Sciences. *Crit. Rev. Solid State Mater. Sci.* **2024**, *49*, 72–140. [CrossRef]
25. Georgakilas, V.; Tiwari, J.N.; Kemp, K.C.; Perman, J.A.; Bourlinos, A.B.; Kim, K.S.; Zboril, R. Noncovalent Functionalization of Graphene and Graphene Oxide for Energy Materials, Biosensing, Catalytic, and Biomedical Applications. *Chem. Rev.* **2016**, *116*, 5464–5519. [CrossRef]
26. Jakus, A.E.; Secor, E.B.; Rutz, A.L.; Jordan, S.W.; Hersam, M.C.; Shah, R.N. Three-Dimensional Printing of High-Content Graphene Scaffolds for Electronic and Biomedical Applications. *ACS Nano* **2015**, *9*, 4636–4648. [CrossRef] [PubMed]

27. Khedekar, V.V.; Mohammed Zaeem, S.; Das, S. Graphene-Metal Oxide Nanocomposites for Supercapacitors: A Perspective Review. *Adv. Mater. Lett.* **2018**, *9*, 2–19. [CrossRef]

28. Ray, S. *Applications of Graphene and Graphene-Oxide Based Nanomaterials*; William Andrew: Norwich, NY, USA, 2015; ISBN 978-0-323-37522-1.

29. Olabi, A.G.; Abdelkareem, M.A.; Wilberforce, T.; Sayed, E.T. Application of Graphene in Energy Storage Device—A Review. *Renew. Sustain. Energy Rev.* **2021**, *135*, 110026. [CrossRef]

30. Kumar, H.; Sharma, R.; Yadav, A.; Kumari, R. Recent Advancement Made in the Field of Reduced Graphene Oxide-Based Nanocomposites Used in the Energy Storage Devices: A Review. *J. Energy Storage* **2021**, *33*, 102032. [CrossRef]

31. Mohammad, A.; Simon, G.P. Rubber-Clay Nanocomposites. In *Polymer Nanocomposites*; Woodhead Publishing Limited: Sawston, UK, 2006; pp. 297–325.

32. Robertson, C.G.; Hardman, N.J. Nature of Carbon Black Reinforcement of Rubber: Perspective on the Original Polymer Nanocomposite. *Polymers* **2021**, *13*, 538. [CrossRef] [PubMed]

33. Qian, M.; Huang, W.; Wang, J.; Wang, X.; Liu, W.; Zhu, Y. Surface Treatment Effects on the Mechanical Properties of Silica Carbon Black Reinforced Natural Rubber/Butadiene Rubber Composites. *Polymers* **2019**, *11*, 1763. [CrossRef] [PubMed]

34. Fan, Y.; Fowler, G.D.; Zhao, M. The Past, Present and Future of Carbon Black as a Rubber Reinforcing Filler—A Review. *J. Clean. Prod.* **2020**, *247*, 119115. [CrossRef]

35. Sankaran, K.; Manoharan, P.; Chattopadhyay, S.; Nair, S.; Govindan, U.; Arayambath, S.; Nando, G.B. Effect of Hybridization of Organoclay with Carbon Black on the Transport, Mechanical, and Adhesion Properties of Nanocomposites Based on Bromobutyl/Epoxidized Natural Rubber Blends. *RSC Adv.* **2016**, *6*, 33723–33732. [CrossRef]

36. Castaño-Rivera, P.; Calle-Holguín, I.; Castaño, J.; Cabrera-Barjas, G.; Galvez-Garrido, K.; Troncoso-Ortega, E. Enhancement of Chloroprene/Natural/Butadiene Rubber Nanocomposite Properties Using Organoclays and Their Combination with Carbon Black as Fillers. *Polymers* **2021**, *13*, 1085. [CrossRef]

37. He, S.J.; Wang, Y.Q.; Lin, J.; Zhang, L.Q. Combined Effect of Nano-Clay and Carbon Black on Mechanical Properties and Aging Resistance of Styrene Butadiene Rubber Nanocomposites. *Adv. Mater. Res.* **2012**, *393–395*, 28–31. [CrossRef]

38. He, S.-J.; Wang, Y.-Q.; Wu, Y.-P.; Wu, X.-H.; Lu, Y.-L.; Zhang, L.-Q. Preparation, Structure, Performance, Industrialisation and Application of Advanced Rubber/Clay Nanocomposites Based on Latex Compounding Method. *Plast. Rubber Compos.* **2010**, *39*, 33–42. [CrossRef]

39. Vasilenko, I.V.; Frolov, A.N.; Kostjuk, S.V. Cationic Polymerization of Isobutylene Using AlCl3OBu2 as a Coinitiator: Synthesis of Highly Reactive Polyisobutylene. *Macromolecules* **2010**, *43*, 5503–5507. [CrossRef]

40. Princi, E. *Rubber: Science and Technology*; Walter de Gruyter GmbH & Co. KG.: Berlin, Germany, 2019; ISBN 978-3-11-064032-8.

41. Tsai, C.-Y.; Lin, S.-Y.; Tsai, H.-C. Butyl Rubber Nanocomposites with Monolayer MoS2 Additives: Structural Characteristics, Enhanced Mechanical, and Gas Barrier Properties. *Polymers* **2018**, *10*, 238. [CrossRef]

42. Sharma, R.K.; Mohanty, S.; Gupta, V. Advances in Butyl Rubber Synthesis via Cationic Polymerization: An Overview. *Polym. Int.* **2021**, *70*, 1165–1175. [CrossRef]

43. Smith, M.; Berlioz, S.; Chailan, J.F. Radiochemical Ageing of Butyl Rubbers for Space Applications. *Polym. Degrad. Stab.* **2013**, *98*, 682–690. [CrossRef]

44. Cao, R.; Zhao, X.; Zhao, X.; Wu, X.; Li, X.; Zhang, L. Bromination Modification of Butyl Rubber and Its Structure, Properties, and Application. *Ind. Eng. Chem. Res.* **2019**, *58*, 16645–16653. [CrossRef]

45. Akiba, M.; Hashim, A.S. Vulcanization and Crosslinking in Elastomers. *Prog. Polym. Sci.* **1997**, *22*, 475–521. [CrossRef]

46. Ciesielski, A. *An Introduction to Rubber Technology*; Smithers Rapra Publishing: Shrewsbury, UK, 1999; ISBN 978-1-85957-150-7.

47. Rodgers, B.; Waddell, W. 9—The Science of Rubber Compounding. In *Science and Technology of Rubber*, 3rd ed.; Mark, J.E., Erman, B., Eirich, F.R., Eds.; Academic Press: Burlington, MA, USA, 2005; pp. 401–454, ISBN 978-0-12-464786-2.

48. Vairon, J.-P.; Spassky, N. Industrial Cationic Polymerizations: An Overview. In *Cationic Polymerizations*; CRC Press: Boca Raton, FL, USA, 1996; ISBN 978-0-429-16842-0.

49. Sukhareva, K.V.; Sukharev, N.R.; Levina, I.I.; Offor, P.O.; Popov, A.A. Solvent Swelling-Induced Halogenation of Butyl Rubber Using Polychlorinated N-Alkanes: Structure and Properties. *Polymers* **2023**, *15*, 4137. [CrossRef] [PubMed]

50. De, S.K.; White, J.R. *Rubber Technologist's Handbook*; Smithers Rapra Publishing: Shrewsbury, UK, 2001; ISBN 978-1-85957-262-7.

51. Ashok, N.; Balachandran, M. Effect of Nanoclay and Nanosilica on Carbon Black Reinforced EPDM/CIIR Blends for Nuclear Applications. *Mater. Res. Express* **2020**, *6*, 125364. [CrossRef]

52. Neelesh, A.; Vidhyashree, S.; Meera, B. The Influence of MWCNT and Hybrid (MWCNT/Nanoclay) Fillers on Performance of EPDM-CIIR Blends in Nuclear Applications: Mechanical, Hydrocarbon Transport, and Gamma-Radiation Aging Characteristics. *J. Appl. Polym. Sci.* **2020**, *137*, 49271. [CrossRef]

53. Su, C.; He, P.; Yan, R.; Zhao, C.; Zhang, C. Study of the Orientation-Controlled Damping Temperature Based on Selective Distribution of Oligo-Phenol in Acrylate Rubber/Chlorinated Butyl Rubber Blends. *Polym. Compos.* **2012**, *33*, 860–865. [CrossRef]

54. Keloth Paduvilan, J.; Velayudhan, P.; Amanulla, A.; Joseph Maria, H.; Saiter-Fourcin, A.; Thomas, S. Assessment of Graphene Oxide and Nanoclay Based Hybrid Filler in Chlorobutyl-Natural Rubber Blend for Advanced Gas Barrier Applications. *Nanomaterials* **2021**, *11*, 1098. [CrossRef] [PubMed]

55. Zachariah, A.K.; Geethamma, V.G.; Chandra, A.K.; Mohammed, P.K.; Thomas, S. Rheological Behaviour of Clay Incorporated Natural Rubber and Chlorobutyl Rubber Nanocomposites. *RSC Adv.* **2014**, *4*, 58047–58058. [CrossRef]

56. Saritha, A.; Joseph, K.; Thomas, S.; Muraleekrishnan, R. Chlorobutyl Rubber Nanocomposites as Effective Gas and VOC Barrier Materials. *Compos. Part Appl. Sci. Manuf.* **2012**, *43*, 864–870. [CrossRef]

57. Sreehari, H.; Aparna, A.; Jayan, J.S.; Sethulekshmi, A.S.; Gopika, V.; Anjali, K.P.; Parvathy, N.; Saritha, A. Evaluation of Solvent Transport and Cure Characteristics of Chlorobutyl Rubber Graphene Oxide Nanocomposites. *Mater. Today Proc.* **2022**, *49*, 1431–1435. [CrossRef]

58. Zhang, F.; He, G.; Xu, K.; Wu, H.; Guo, S.; Zhang, C. Damping Mechanism and Different Modes of Molecular Motion through the Glass Transition of Chlorinated Butyl Rubber and Petroleum Resin Blends. *J. Appl. Polym. Sci.* **2014**, *131*, 40464. [CrossRef]

59. Kraus, G. Degree of Cure in Filler-Reinforced Vulcanizates by the Swelling Method. *Rubber Chem. Technol.* **1957**, *30*, 928–951. [CrossRef]

60. Picard, E.; Espuche, E.; Fulchiron, R. Effect of an Organo-Modified Montmorillonite on PLA Crystallization and Gas Barrier Properties. *Appl. Clay Sci.* **2011**, *53*, 58–65. [CrossRef]

61. Bordes, P.; Pollet, E.; Avérous, L. Nano-Biocomposites: Biodegradable Polyester/Nanoclay Systems. *Prog. Polym. Sci.* **2009**, *34*, 125–155. [CrossRef]

62. Hummers, W.S., Jr.; Offeman, R.E. Preparation of Graphitic Oxide. *J. Am. Chem. Soc.* **1958**, *80*, 1339. [CrossRef]

63. Capezza, A.; Andersson, R.L.; Ström, V.; Wu, Q.; Sacchi, B.; Farris, S.; Hedenqvist, M.S.; Olsson, R.T. Preparation and Comparison of Reduced Graphene Oxide and Carbon Nanotubes as Fillers in Conductive Natural Rubber for Flexible Electronics. *ACS Omega* **2019**, *4*, 3458–3468. [CrossRef] [PubMed]

64. Dal Lago, E.; Cagnin, E.; Boaretti, C.; Roso, M.; Lorenzetti, A.; Modesti, M. Influence of Different Carbon-Based Fillers on Electrical and Mechanical Properties of a PC/ABS Blend. *Polymers* **2020**, *12*, 29. [CrossRef] [PubMed]

65. Zhao, S.; Zhao, H.; Li, G.; Dai, K.; Zheng, G.; Liu, C.; Shen, C. Synergistic Effect of Carbon Fibers on the Conductive Properties of a Segregated Carbon Black/Polypropylene Composite. *Mater. Lett.* **2014**, *129*, 72–75. [CrossRef]

66. Clingerman, M.L.; Weber, E.H.; King, J.A.; Schulz, K.H. Synergistic Effect of Carbon Fillers in Electrically Conductive Nylon 6,6 and Polycarbonate Based Resins. *Polym. Compos.* **2002**, *23*, 911–924. [CrossRef]

67. Vipulanandan, C.; Mohammed, A. Effect of Nanoclay on the Electrical Resistivity and Rheological Properties of Smart and Sensing Bentonite Drilling Muds. *J. Pet. Sci. Eng.* **2015**, *130*, 86–95. [CrossRef]

68. Rajini, N.; Jappes, J.T.W.; Rajakarunakaran, S.; Poornanand, P. Electrical Properties of Montmorillonite Nanoclay Reinforced Unsaturated Polyester Nanocomposite. In Proceedings of the IEEE-International Conference On Advances In Engineering, Science And Management (ICAESM-2012), Nagapattinam, India, 30–31 March 2012.

69. Rashmi; Renukappa, N.M.; Chikkakuntappa, R.; Kunigal, N.S. Montmorillonite Nanoclay Filler Effects on Electrical Conductivity, Thermal and Mechanical Properties of Epoxy-Based Nanocomposites. *Polym. Eng. Sci.* **2011**, *51*, 1827–1836. [CrossRef]

70. Bauhofer, W.; Kovacs, J.Z. A Review and Analysis of Electrical Percolation in Carbon Nanotube Polymer Composites. *Compos. Sci. Technol.* **2009**, *69*, 1486–1498. [CrossRef]

71. Mott, S.N.F.; Davis, E.A. *Electronic Processes in Non-Crystalline Materials*; OUP Oxford: Oxford, UK, 2012; ISBN 978-0-19-964533-6.

72. Yang, Y.; Sun, H.; Zhu, B.; Wang, Z.; Wei, J.; Xiong, R.; Shi, J.; Liu, Z.; Lei, Q. Enhanced Dielectric Performance of Three Phase Percolative Composites Based on Thermoplastic-Ceramic Composites and Surface Modified Carbon Nanotube. *Appl. Phys. Lett.* **2015**, *106*, 012902. [CrossRef]

73. Vorobiev, A.; Dennison, A.; Chernyshov, D.; Skrypnychuk, V.; Barbero, D.; Talyzin, A.V. Graphene Oxide Hydration and Solvation: An in Situ Neutron Reflectivity Study. *Nanoscale* **2014**, *6*, 12151–12156. [CrossRef]

74. Rezania, B.; Severin, N.; Talyzin, A.V.; Rabe, J.P. Hydration of Bilayered Graphene Oxide. *Nano Lett.* **2014**, *14*, 3993–3998. [CrossRef]

75. Pei, S.; Zhao, J.; Du, J.; Ren, W.; Cheng, H.-M. Direct Reduction of Graphene Oxide Films into Highly Conductive and Flexible Graphene Films by Hydrohalic Acids. *Carbon* **2010**, *48*, 4466–4474. [CrossRef]

76. Vallés, C.; David Núñez, J.; Benito, A.M.; Maser, W.K. Flexible Conductive Graphene Paper Obtained by Direct and Gentle Annealing of Graphene Oxide Paper. *Carbon* **2012**, *50*, 835–844. [CrossRef]

77. Yao, Y.; Chen, X.; Zhu, J.; Zeng, B.; Wu, Z.; Li, X. The Effect of Ambient Humidity on the Electrical Properties of Graphene Oxide Films. *Nanoscale Res. Lett.* **2012**, *7*, 363. [CrossRef] [PubMed]